Advances in Biological Regulation xxx (xxxx) xxx–xxx

Contents lists available at ScienceDirect

Advances in Biological Regulation

journal homepage: www.elsevier.com/locate/jbior

Crosstalk between Ras and inositol phosphate signaling revealed by lithium action on inositol monophosphatase in *Schizophyllum commune*

Reyna Murry[a], Olaf Kniemeyer[b], Katrin Krause[a], Adolfo Saiardi[c,**], Erika Kothe[a,*]

[a] *Friedrich Schiller University Jena, Institute of Microbiology, Jena, Germany*
[b] *Leibniz Institute for Natural Product Research and Infection Biology - Hans Knöll Institute Jena, Germany*
[c] *Medical Research Council (MRC) Laboratory for Molecular Cell Biology, Department of Biochemistry and Molecular Biology, University College London, London, UK*

ARTICLE INFO

Keywords:
Inositol phosphates
Signaling
Inositol monophosphatase
IMPA
Ras
lithium
Schizophyllum commune
basidiomycete fungi

ABSTRACT

Mushroom forming basidiomycete *Schizophyllum commune* has been used as a tractable model organism to study fungal sexual development. Ras signaling activation *via* G-protein-coupled receptors (GPCRs) has been postulated to play a significant role in the mating and development of *S. commune*. In this study, a crosstalk between Ras signaling and inositol phosphate signaling by inositol monophosphatase (IMPase) is revealed. Constitutively active Ras1 leads to the repression of IMPase transcription and lithium action on IMPase activity is compensated by the induction of IMPase at transcriptome level. Astonishingly, in *S. commune* lithium induces a considerable shift to inositol phosphate metabolism leading to a massive increase in the level of higher phosphorylated inositol species up to the inositol pyrophosphates. The lithium induced metabolic changes are not observable in a constitutively active Ras1 mutant. In addition to that, proteome profile helps us to elucidate an overview of lithium action to the broad aspect of fungal metabolism and cellular signaling. Taken together, these findings imply a crosstalk between Ras and inositol phosphate signaling.

1. Introduction

Inositol based signaling pathways are between the most complex regulatory networks present in eukaryotic cells. The phosphatidylinositol (PI) signaling cascade and the rapid turnover of inositol phosphates by kinases and phosphatases regulate a wide range of cellular activities (Irvine and Schell, 2001; Di Paolo and Camilli, 2006; Wilson et al., 2013). The most polar inositol phosphates (IPs) species, the inositol pyrophosphates IP7 and IP8, are able to regulate basic metabolism (Szijgyarto et al., 2011) thanks to their ability to control phosphate homeostasis (Lonetti et al., 2011; Saiardi, 2012; Wild et al., 2016; Azevedo and Saiardi, 2017). In mammals, inositol signaling regulates neuronal development (Zhang et al., 2017) and affects the physiology of important illnesses such as bipolar disorder (Saiardi and Mudge, 2018) and Alzheimer diseases (Crocco et al., 2016). In plants, inositol signaling is important for drought or salt resistance (Li et al., 2017; Pan et al., 2017), response to phytopathogen attack (Gupta et al., 2017), or mycorrhization (Nanjareddy et al., 2017). The budding yeast *Saccharomyces cerevisiae* is easyly genetically manipulated to permit discovery of additional IPs functions. Fundamental physiological processes are regulated by IPs, including transcription (Hatch et al.,

* Corresponding author. Friedrich Schiller University, Institute of Microbiology, Neugasse 25, 07743, Jena, Germany.
** Corresponding author. MRC University College London, Laboratory for Molecular Cell Biology, Gower Street, London, WC1E 6BT, UK.
E-mail addresses: a.saiardi@ucl.ac.uk (A. Saiardi), erika.kothe@uni-jena.de (E. Kothe).

https://doi.org/10.1016/j.jbior.2019.01.001
Received 12 December 2018; Received in revised form 31 December 2018; Accepted 2 January 2019

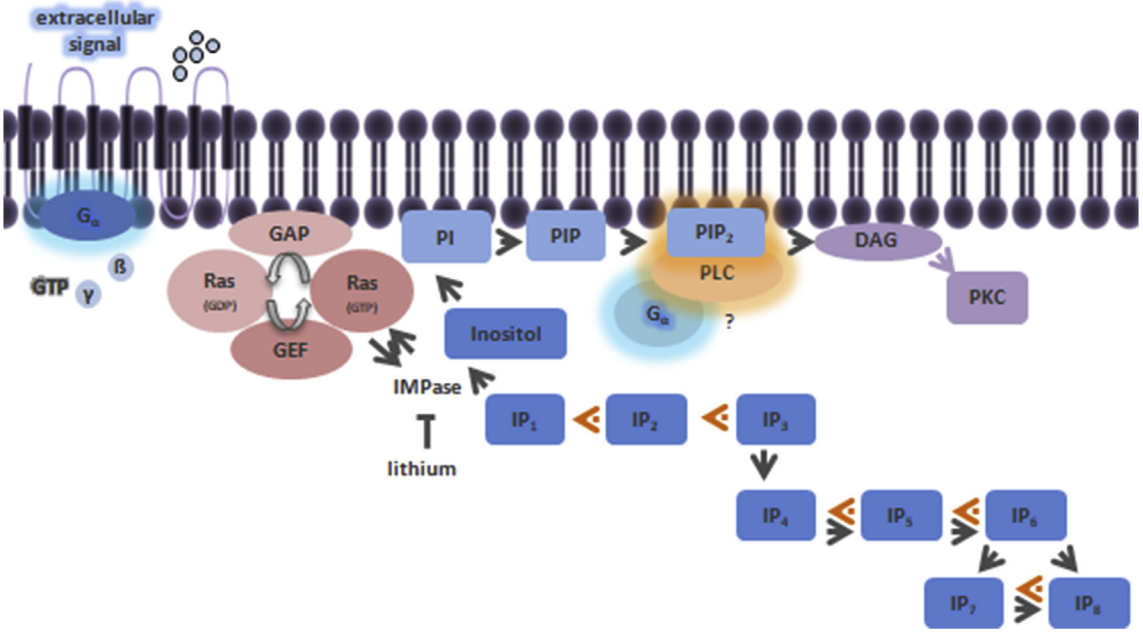

Fig. 1. Inositol phosphate (IP) signaling pathway in *S. commune*. The binding of extracellular stimuli to G-alpha subunit (G_α) activates subsequently phospholipase C (PLC). PLC cleaves phosphatidylinositol (PI)-4,5-bisphosphate (PIP_2) generating 2 s messengers, inositol 1,4,5 triphosphate (IP_3), shuttling between higher phosphorylated inositol phosphate (IP_4 to IP_8) and regenerating inositol through IP_2 and IP_1, and diacylglycerol (DAG) activating protein kinase C (PKC). The lithium sensitive and Ras-regulated inositol monophosphatase (IMPase) generates inositol from inositol monophosphate (IP_1). The Ras module with its guanosin exchange factor (GEF) and its GTPas activating protein (GAP) is shown. Inositol is used to build up phosphoinositides (PI; PIP; PIP_2) and inositol phosphates using inositol phosphate kinases (black arrow) and phosphatases (dashed orange arrow).

2017) and the cell cycle (Banfic et al., 2016). The simple yeast IPs metabolism is shared by the majority of microorganism including important human pathogens such as *Trypanosoma* (Cordeiro et al., 2017) and *Cryptococcus neoformans* (Lev et al., 2015). The presence of a more complex and likely redundant IPs metabolism in humans advocates for the microbial IPs metabolic pathway to be used as a potential drug development target (Saiardi et al., 2018).

Phosphoinositides, integrated into membranes, are involved in calcium spiking and oscillation (Berridge et al., 1982) and in determining membrane identity and intracellular trafficking (Hammond and Balla, 2015; De Craene et al., 2017). PI signaling (Fig. 1) depends on inositol supply to generate phosphatidylinositol bisphosphate (PIP_2) the substrate of phospholipase-C (PLC; Gillaspy, 2011). Upon activation of a G-protein coupled receptor or receptor tyrosine kinase, PLC generates the cytosolic second messenger inositol triphosphate (IP_3). Through a phosphorylation cascade, more polar IPs are synthesized. However, IP_3 is mainly recycled back to inositol, for re-starting the PI cycle. Key to recycle IP_3 is inositol monophosphatase (IMPase), an enzyme that converts inositol monophosphate (IP_1) to inositol (Tsui and York, 2010).

Mammals possess two IMPase genes, *impa1 and impa2*. Deletin of *impa1* in mice revealed that this gene is essential in mouse embryogenesis (Cryns et al., 2008). Also plants and the yeast *S. cerevisiae* possess multiple IMPase genes (Navarro-Aviñó et al., 2003; Nourbakhsh et al., 2015.). The repression of this enzyme can be studied using lithium that acts as inhibitor for IMPase gene family enzymes (York and Majerus, 1990). The competitive inhibition by lithium has led to the inositol depletion hypothesis, which was proposed as the main effect of lithium in treating bipolar disorder patients (Saiardi, 2018; Allison and Stewart, 1971; Berridge, 1989). Thus, IMPase has a pivotal role in regulating the flux of inositol through the de-phosphorylation cycle (see Fig. 1).

The inositol depletion hypothesis acting through lithium inhibition of IMPase should theoretically lead to higher levels of IP_3, which is no longer recycled back to inositol. In consequence, a tailback should be expected with increased levels of highly phosphorylated inositol phosphates IP_4 through IP_6 and the derived inositol pyrophosphates IP_7 and IP_8. However, the increase in higher inositol phosphate species could not be observed using mammalian, plant, or yeasts experimental models (neither with the ascomycete yeasts *S. cerevisiae* or *Schizosaccharomyces pombe,* nor the basidiomycetous yeast form of *C. neoformans;* Lev et al., 2015). Rather, in these organisms the inhibition of IMPase by lithium showed an accumulation of IP_1, and sometimes of inositol bisphosphate (IP_2; Saiardi and Mudge, 2018; Sherman et al., 1981).

Filamentous fungi have not yet been used to address inositol signaling with the exception of the ascomycete *Podospora anserina* (Xie et al., 2017). Filamentous, mushroom forming basidiomycetes, however, are well suited to appreciate IPs functions in phosphate homeostasis and signaling pathways. First, hyphae are prone to experience high phosphate levels in separate places in their environment and are capable to use it for the growth of other hyphae at a distance through transport within the mycelium. Hence, transport and storage of phosphate have been selected for during evolution in filamentous fungi. Second, the read-out for inositol based signaling is not compromised by variable answers in different tissues or highly regulated developmental processes. Fungi are

fully able to grow as haploid mycelia, and even after mating, a dikaryotic stage with the two separate nuclei ensues that enables to identify directly the result of inositol based signaling and single gene mutations.

Schizophyllum commune has been selected to study the tetrapolar mating system (Kothe, 1999; Palmer and Horton, 2006; Ohm et al., 2010), which involves pheromone perception and subsequent intracellular signaling through cyclic adenosine monophosphate (cAMP), mitogen-activated protein kinase (MAPK) and Ras signaling. Inactivation of *gap1,* the negative regulator for the small GTPase Ras1, or introduction of a constitutively active Ras allele has been shown to impact polarized hyphal growth, fruiting body development, and sporulation (Schubert et al., 2006). Microarray analyses revealed a high level of repression of IMPase gene transcription (Knabe et al., 2013). Since inositol monophosphatase generates inositol from IP_1 for a new round of signal perception and intracellular signal transduction *via* inositol phosphates, the evidence suggests an involvement of IPs signaling in sexual development.

In this study, we assessed the effect of lithium and the involvement of Ras1 in inositol phosphate signaling of *S. commune*. With this approach, we could verify the expected, but until now, elusive high phosphorylated inositol phosphates accumulation upon lithium inhibition of IMPase enzyme, and uncovered a cross-talk between Ras and inositol phosphate signaling.

2. Material and methods

2.1. Fungal cultivation, growth rate measurement, and microscopy

Fungal strains were obtained from the Jena Microbial Resource Collection (JMRC, Jena, Germany; suppl. Table S3). CYM (Schwalb and Miles, 1967) solid media were used for cultivation with or without 5 mM lithium chloride and 5 mM potassium chloride (as a salt control). The growth rate was calculated from mycelial extension rates based on three replicates of mycelia diameter measurements. Significant differences were confirmed by Student's t-test (p-value ≤ 0.05).

For microscopy, *S. commune* was inoculated on solid CYM covered with a sterile cover slip, and mycelia were microscopically examined (Axioplan2, Carl Zeiss MicroImaging, Jena, Germany). Images were taken with the digital camera Insight Firewire 4 image sample (Diagnostic Instruments, Sterling Heights, MI) and processed with SPOT imaging software (Zeiss, Jena, Germany).

2.2. IMPase activity measurements

IMPase activity was determined as the lithium-sensitive phosphate release measured using the malachite green assay (Baykov et al., 1988; Kalujnaia et al., 2010). Five days old liquid cultures of *S. commune* were ground using liquid nitrogen and subsequently extracted using 4 ml protein extraction buffer (25 mM Tris/HCl, 1 mM DTT, 1 mM EDTA, pH 7.4) added to 1 g of mycelial powder followed by incubation on ice for 15 min and centrifugation at 14,000 rpm at 4 °C for 10 min (Mikro200R, Hettich Zentrifugen, Tuttlingen, Germany). Inorganic phosphate (P_i) standard (Na_2HPO_4, 0–100 nmol/ml) and protein extract diluted to 1 µg/ml protein in buffer A (25 mM HEPES, 0.25 M sucrose, 2 mM $MgCl_2$, pH 7.4 containing protease inhibitor cocktail for yeast and fungal extracts; Sigma Aldrich, Hamburg, Germany) with or without LiCl (50 mM) mixed 1:1, incubated on ice for 10 min and added to a 96 well-plate. 90 µl of buffer B (25 mM HEPES, 2 mM $MgCl_2$, 200 µM inositol phosphate, pH 7.4) was added, the reaction mix incubated for 60 min at room temperature (RT) and stopped by adding 50 µl of Malachite Green reagent (Baykov et al., 1988). Maximum absorption was determined at a wavelength of 640 nm (Ultrospect™ 2100 Pro UV/Visible Spectrophotometer, Amersham Biosciences, Freiburg, Germany).

2.3. RNA extraction, cDNA synthesis and qRT-PCR

The fungus was cultivated on a sterile cellophane membrane placed on top of CYM solid media for 5 days at 28 °C. The recovered mycelium was ground with pestle and mortar in liquid nitrogen and 100 mg used for RNA extraction (Qiagen RNeasy plant mini kit, QIAGEN, Hilden, Germany). Reverse transcription from 500 ng total RNA (Quantitect Reverse Transcription Kit, QIAGEN, Hilden, Germany) was followed by quantitative real-time PCR using 12.5 µl Maxima SYBR Green/ROX qPCR Master mix (Thermo Fisher Scientific, Hamburg, Germany), 1 µl forward and reverse primers (10 pmol/µl of each, Eurofins, Hamburg, Germany; see suppl. Tab. S4), 9.5 µl PCR grade water (Prime, Hamburg, Germany), and 2 µl of 50 ng/µl cDNA (Cepheid tubes, Sunnyval, USA). Fluorescence was detected (excitation wavelength 450–495 nm, emission wavelength 510–527 nm) from three biological replicates and with three technical replicates for each gene. Relative quantification of gene expression was normalized to the reference gene *tef1* (JGI ID Schco3 84142) and PCR efficiency was corrected as described (Pfaffl, 2001).

2.4. Inositol phosphates detection

Inositol phosphates extraction was performed as described previously (Azevedo and Saiardi, 2006) with several modifications. Mycelia were grown in 100 ml minimal medium containing 10 mM uracil (MMura) for the auxotrophic strain (Raper and Miles, 1958). The mycelia were homogenized with fresh MMura (1:1) using a laboratory blender (Waring, Torrington, USA), and 3 ml of diluted culture was labeled with 15 µl of myo-[2–^{3}H(N)]-inositol (1 mCi/ml; Perkin Elmer, USA) for 24 h. The labeled mycelia were passed 10 times through an 18G needle and pelleted at 4000 rpm for 5 min. After washing with ultrapure water twice and pelleting at 14,000 rpm for 5 min, soluble inositol phosphates were extracted using 500 µl freshly made extraction solution (1 M $HClO_4$, 5 mM EDTA) and 500 µl of glass beads. The mixture was vigorously disrupted using a cell disruptor (Digital Disruptor Genie, Scientific

Industries, USA) for 10 min and centrifuged at 4 °C, 14,000 rpm for 5 min. The liquid phase containing the soluble inositol phosphates was transferred to a new 1.5 ml tube, neutralized using freshly made neutralization buffer (1 M K_2CO_3, 5 mM EDTA), and incubated on ice for 2 h while the cap remained open. The tube was flipped every 15 min and centrifuged at 4 °C, 14,000 rpm for 5 min. The supernatant containing inositol phosphates was transferred to a new tube without disturbing the pellet and analyzed by Strong Anion Exchange (SAX) HPLC (SAX 4.6 × 125 mm column; Hichrom, UK). The column was eluted by mixing buffer A (1 mM Na_2EDTA) and buffer B (1 mM EDTA; 1.3 M $(NH_4)_2HPO_4$, pH 3.8 with H_3PO_4) as follows: 0–5 min, 0% buffer B; 5–10 min, 0–10% buffer B; 10–75 min, 10–100% buffer B; 75–85 min, 100% buffer B; 85–86 min, 0% buffer B; 86–96 min, 0% buffer B. Four ml of Ultima-Flo AP liquid scintillation cocktail (Perkin-Elmer, MA, USA) was added to each fraction and radioactivity quantified in a scintillation counter (Beckman Coulter, USA).

2.5. Proteome analysis

Cytosolic protein isolation was performed as described previously (Bordier, 1981). Five days after inoculation, mycelia were ground with mortar and pestle in liquid nitrogen. 25 ml of solution A (80 mM Tris-HCl, pH 7.4, 1.2 M NaCl) and 10 ml of solution B (40 mM Tris-HCl, pH 7.4, 0.6 M NaCl, and 4% Triton X-114) were added to 5 g of mycelia powder, incubated on ice for 1 h and centrifuged at 11,000 rpm, 4 °C for 15 min. The supernatant was incubated in a new reaction tube for 3 min at 30 °C, and centrifuged at 1600 rpm, RT for 10 min (Rotina 380 R, Hettich, Tuttlingen, Germany). The aqueous phase was added to 1 volume of precipitation buffer (20% TCA, 50% acetone) and incubated overnight at 4 °C. The precipitate was centrifuged (11,000 rpm, 4 °C for 10 min), the pellet washed 4 times with pure acetone, and dried. Using 1 ml of rehydration buffer (8 M urea, 2 M thiourea, 4% CHAPS) followed by centrifugation (13,000 rpm, 4 °C for 10 min), the protein was dissolved and the concentration determined (Bradford, 1976). Using 250 µg protein for rehydration (Immobiline DryStrip pH 3–7; pH 3–11, 24 cm, GE Healthcare, Uppsala, Sweden) with 2% (v/v) IPG buffer (pH 3–11) and 5.4 µl of DeStreak reagent (GE Healthcare, Uppsala, Sweden) in a volume adjusted to 450 µl with rehydration buffer, the samples were transferred to a reswelling tray (GE, Healthcare, Uppsala, Sweden) for 20–24 h, at RT. Proteins were separated in the first dimension according to their isoelectric point (Ettan IGPhor II, GE Healthcare, Uppsala, Sweden) covered with Immobiline DryStrip cover fluid (GE Healthcare, Uppsala, Sweden) and run at 300 V for 4 h (gradient), 600 V for 4 h (gradient), 1000 V for 4 h (gradient), 8000 V for (gradient) and 8000 V for 24000 Vhr (step).

The strips were incubated in equilibration buffer 1 (6 M urea, 2% SDS, 30% glycerin, 3.3% separating buffer, 1% DTT) and equilibration buffer 2 (6 M urea, 2% SDS, 30% glycerin, 3.3% separating buffer, 24% iodoacetamide) for 15 min each, loaded on top of 10% (w/v) polyacrylamide gel and electrophoresis was performed (Ettan DALTtwelve, GE Healthcare, Uppsala, Sweden) in 1x running buffer in the lower chamber and 2x running buffer in the upper chamber at 1 W per gel for 1 h and at 15 W per gel for 8–10 h. After electrophoresis, gels were fixed for 30 min (40% methanol, 7% acetic acid) and stained (20% methanol, 2% *o*-phosphoric acid, 10% ammonium sulfate, 0.1% Coomassie Brilliant Blue G-250) overnight, neutralized (Tris HCl pH 6.5 for 10 min) destained (25% methanol) and scanned (Epson Bio Step ViewPix scanner, Biostep, Burkhardtsdorf, Germnay). Images were analyzed using Delta2D imaging software v. 4.3 (Decodon, Greifswald, Germany).

Differential spots were excised, eluted (Brunsch et al., 2015) and protein identification was performed using MALDI TOF/MS after tryptic digestion (Shevchenko et al., 1996) using 1 µl HCCA matrix (10 mg/ml alpha cyano-4-hydroxy-cinnamic acid in 30% acetonitrile, 70% distilled water with 0.1% trifluoroacetic acid) transferred to an Anchor Chip Target (Bruker Daltonics, Bremen) for 1 µl of the tryptically digested sample. The dried samples were analyzed (ultrafleXtreme MALDI-TOF/TOF; Bruker, Bremen, Germany) and measured using flexControl software followed by analysis with flexAnalysis. Peptides were identified from the *S. commune* genome (JGI database *S. commune* v3.0) using oxidized methionine as variable modification, carbamidomethyl cysteine as fixed modification, one missed cleavage, a peptide mass tolerance of 100 ppm and a fragment mass tolerance of 0.6 Da. Significant results were determined with an allowed likelihood for a random hit of p-value ≤ 0.05, according to the Mascot score.

3. Results

3.1. IMPase expression is under control of Ras and function can be inhibited by lithium chloride

In order to verify the repression of *imp1* by activated Ras signaling, qRT-PCR was performed using Ras activated *S. commune* $ras1^{G12V}$ and wild-type strains. Since IMPase is a lithium sensitive enzyme, the effect of 5 mM LiCl on *imp* gene expression was also included. The gene *imp1* was strongly repressed upon Ras1 activation (52-fold transcriptional repression; Fig. 2) and in the deletion mutant lacking the GTPase-activating protein Gap1 (35-fold repression; Erdmann et al., 2012). Interestingly, lithium further repressed *imp1* expression in $ras1^{G12V}$, while it did not affect *imp1* expression in the wild type. These data triggered us to examine the effect of lithium on the IMPase enzymatic activity. IMPase enzyme activity in the wild type was on average more than 2-fold higher compared to the constitutive active $ras1^{G12V}$ (Fig. 2). Conversely, lithium reduced IMPase activity by 20% and 60% in the wild type and in the constitutively active Ras1 mutant, respectively.

The growth rate on CYM solid medium supplemented with 5 mM LiCl was significantly reduced in the wild type (55%; Fig. 3), while the growth of *S. commune* $ras1^{G12V}$ appeared to be only marginally inhibited. The growth repression by LiCl was correlated with altered colony and hyphal morphology, while KCl exerted no changes (see Fig. 3). The growth and morphology in the $ras1^{G12V}$ mutant were not affected significantly in the presence of 5 mM LiCl.

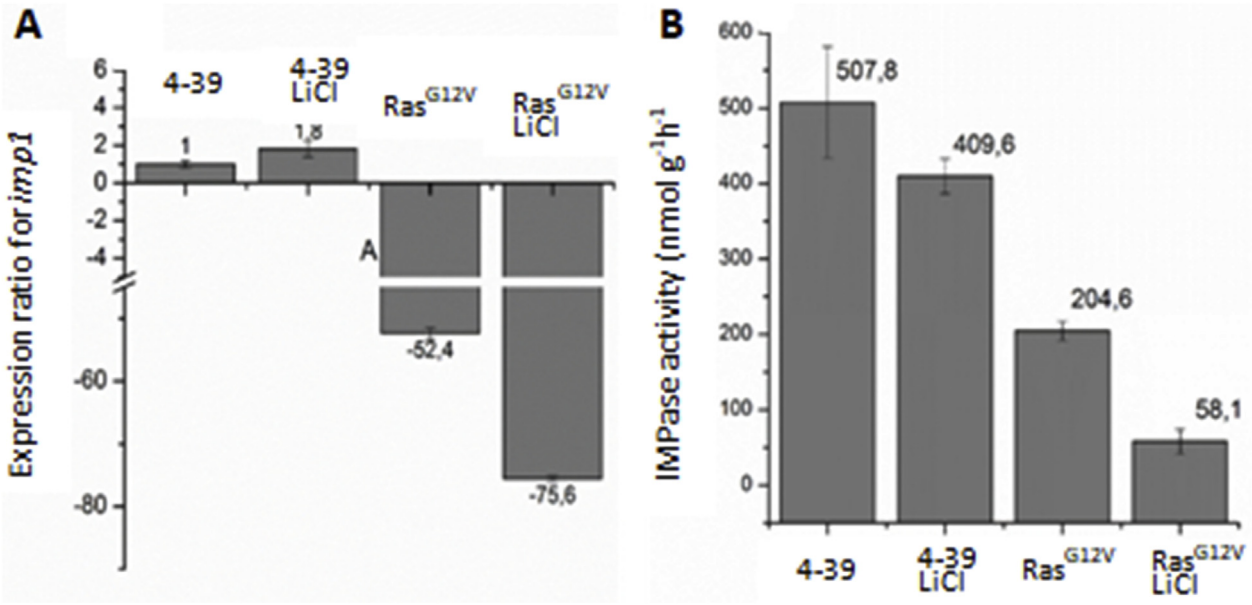

Fig. 2. Expression of *imp1*. Expression levels on transcript (A) and IMPase enzyme activity (B) were tested for the wild type *S. commune* 4–39 and constitutively active Ras1 mutant *S. commune* $ras1^{G12V}$. Lithium was tested for *imp1* gene induction, counter-acting enzyme repression; *tef1* was used as reference gene.

3.2. Inositol phosphates were increased upon reduction of IMPase activity

The growth inhibitory effect of lithium and the striking transcriptional control executed by Ras signaling on *imp1* prompted us to investigate the biochemical consequence of lithium treatment in *S. commune*. We labeled *S. commune* with [^{3}H]-inositol and then resolved the IPs on SAX-HPLC. This analysis revealed an elution profile comparable to that of the bakers' yeast *S. cerevisiae* (Saiardi et al., 2002) or the basidiomycete yeast form of *C. neoformans* (Lev et al., 2015), with inositol hexakisphosphate (IP_6) as the most abundant species (Fig. 4). The slow growth of the strain harboring $ras1^{G12V}$ led to a generally reduced accumulation of [^{3}H]-inositol into IPs with elution profiles similar between 48 h in the mutant and 24 h in the wild type (suppl. Fig. S1).

Lithium treatment (5 mM LiCl for 24 h) in the wild type showed a decrease in IP_1 level. Extraordinarily, we observed a 2- to 4-fold increase in higher phosphorylated IPs species, including the inositol pyrophosphates IP_7 and IP_8 (Fig. 4). The species with the highest increase was IP_6, where we observed on average 4.3 ± 1.8 (± SD; n = 3) -fold increase upon lithium treatment. On the contrary, lithium had no significant effect on the inositol phosphates elution profile of constitutively active $ras1^{G12V}$ mutant either for 24 or 48 h treatment (see suppl. Fig. S1).

3.3. Lithium changes the cytosolic protein profile of S. commune

In order to identify pathways and/or protein targets regulated upon lithium treatment, 2D-PAGE was performed and followed by mass spectrometry analyses. Proteins were isolated from the wildtype and the $ras1^{G12V}$ mutant, cultivated in presence or absence of lithium (Fig. 5; suppl. Tabs. S1, S2; suppl. Figs. S2 and S3). Proteins with change in abundance were identified by MS and functional assignment was performed using the KOG (EuKaryotic Orthologous Groups) classification. The KOG group assignment showed a metabolic shift upon IMPase activity reduction associated with cellular processes/signaling and information storage/processing, while 26 repressed and 29 induced proteins responded to lithium in *S. commune* $ras1^{G12V}$ (Fig. 5). Histidine acid phosphatase (HAP; JGI protein ID 1135584) was repressed by lithium in the wildtype, but induced in the Ras1 constitutively active mutant (ID 2643503). HAP is a conserved signature present in inositol phosphate phosphatases and catalyzes the hydrolysis of IP_6 to inositol (Wyss et al., 1999; Mullaney and Ullah, 2005). Repression of HAP occurred only in the wild type, which correlated with the increase in higher phosphorylation of inositol phosphates seen with lithium treatment.

Fructose 1,6-bisphosphate aldolase and fructose-1,6-bisphosphatase are repressed by lithium in both the wild type and active Ras1 mutant. Since fructose-1,6-bisphosphatase belongs to the metal-dependent and lithium-sensitive phosphomonoesterase protein family, which also includes inositol monophosphatase and inositol polyphosphate 1-phosphatase (York et al., 1995), protein levels of the inactivated enzymes seems to be prone to undergo proteolysis. Surprisingly, we have found that cytoskeleton protein actin-1 (IDs 1194206 and 2645649, in the wild type and active Ras1 mutant, respectively) are repressed in the lithium treatment in both strains, which implies that lithium may have an effect on actin dynamics, taking into account the importance of actin in the polar hyphal growth.

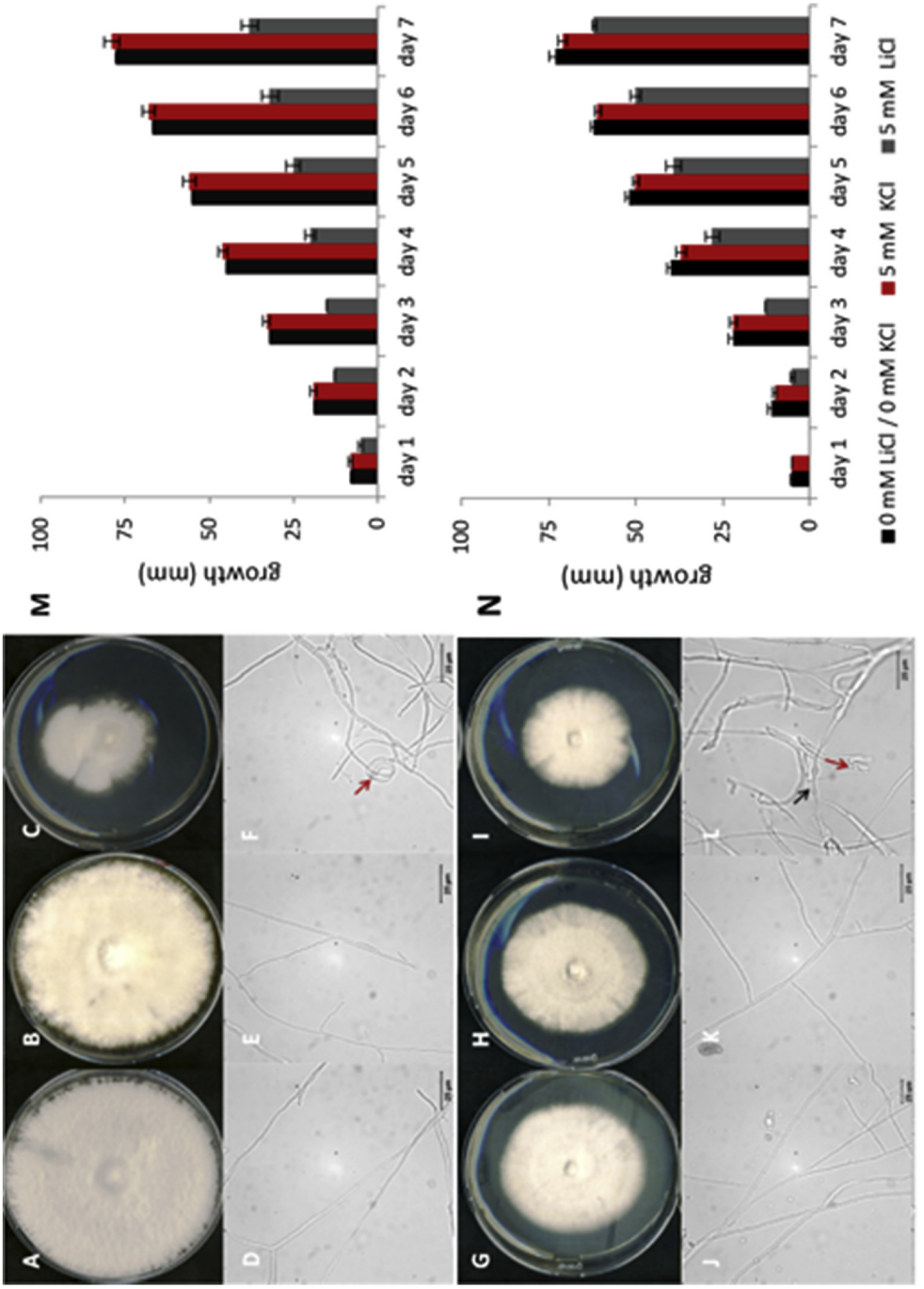

Fig. 3. Influence of lithium on colony and hyphal morphology, and on growth rates. *S. commune* 4–39 (A–F) and constitutively active Ras1 mutant *S. commune* $ras1^{G12V}$ (G–L) were screened after 7 days for the effects of 5 mM LiCl (C, F, I, L) or KCl (B, E, H, K); red arrows show irregular hyphae; black arrow shows bulbous or swollen hyphae. Growth rates of *S. commune* 4–39 (M) and *S. commune* $ras1^{G12V}$ (N) were measured; n = 3.

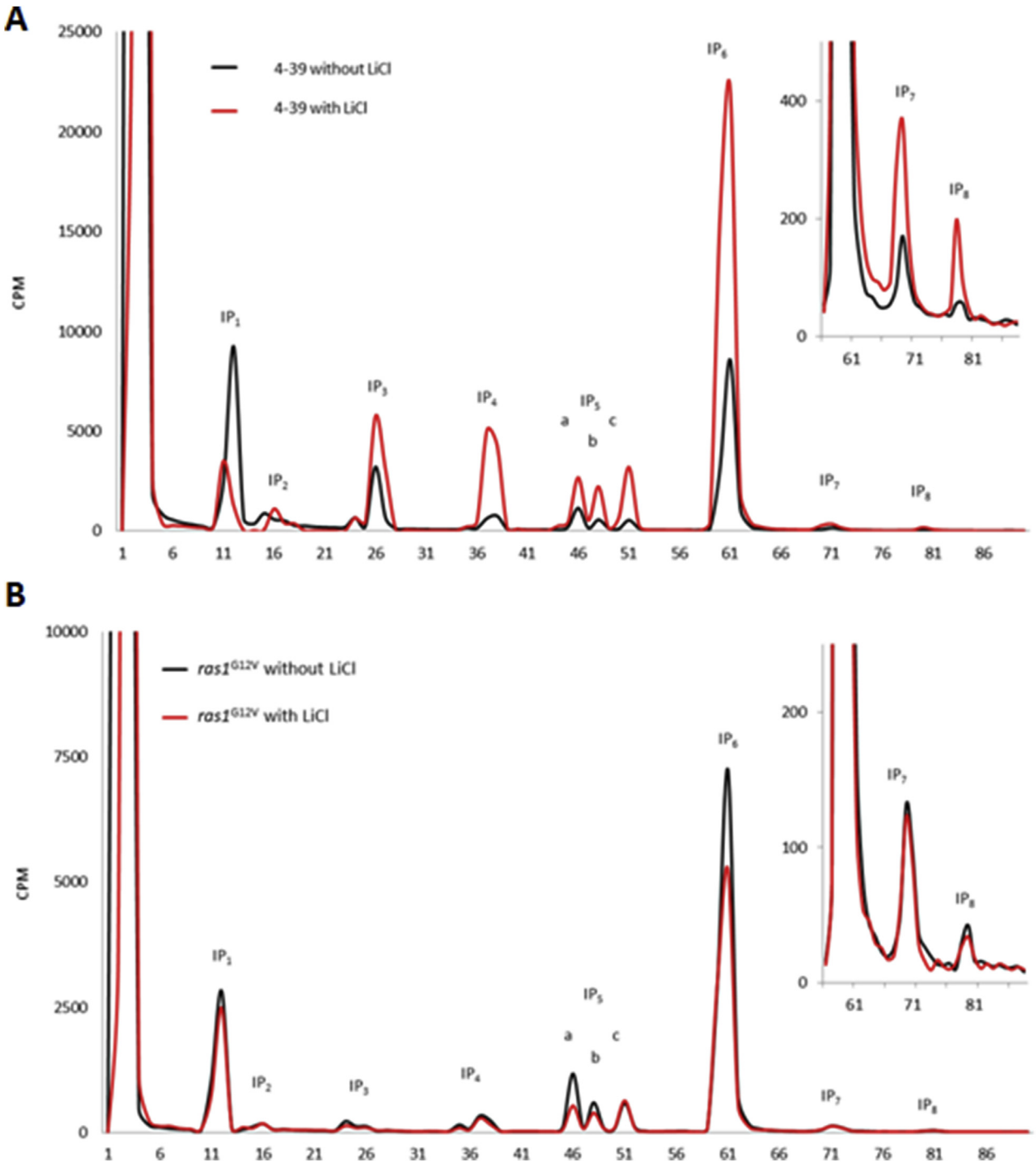

Fig. 4. Effect of lithium on the inositol phosphates profile of wildtype *S. commune* 4–39 and constitutively active *S. commune* Ras1^{G12V} mutant. Chromatographic elution profile of soluble inositol phosphates of *S. commune* wild type 4–39 (A) and constitutive active Ras1^{G12V} mutant (B). Mycelia were labeled 24 h in absence (black trace) or presence of lithium (red trace) as described in material and methods, before extraction and SAX-HPLC analysis. To reveal changes in the inositol pyrophosphate IP_7 and IP_8, the chromatogram was presented in a different scale (inset). Elution time of genuine standard (IP_3, [^{3}H]I(1,4,5)P_3; IP_6, [^{3}H]IP_6; IP_7, [^{3}H]PP-IP5) was used for peak identification. Of the three IP_5 species identified in *S. commune,* $IP5_a$ was identified as [^{3}H]I(1,3,4,5,6)P_5. The elution profile is representative of experiments independently repeated three times.

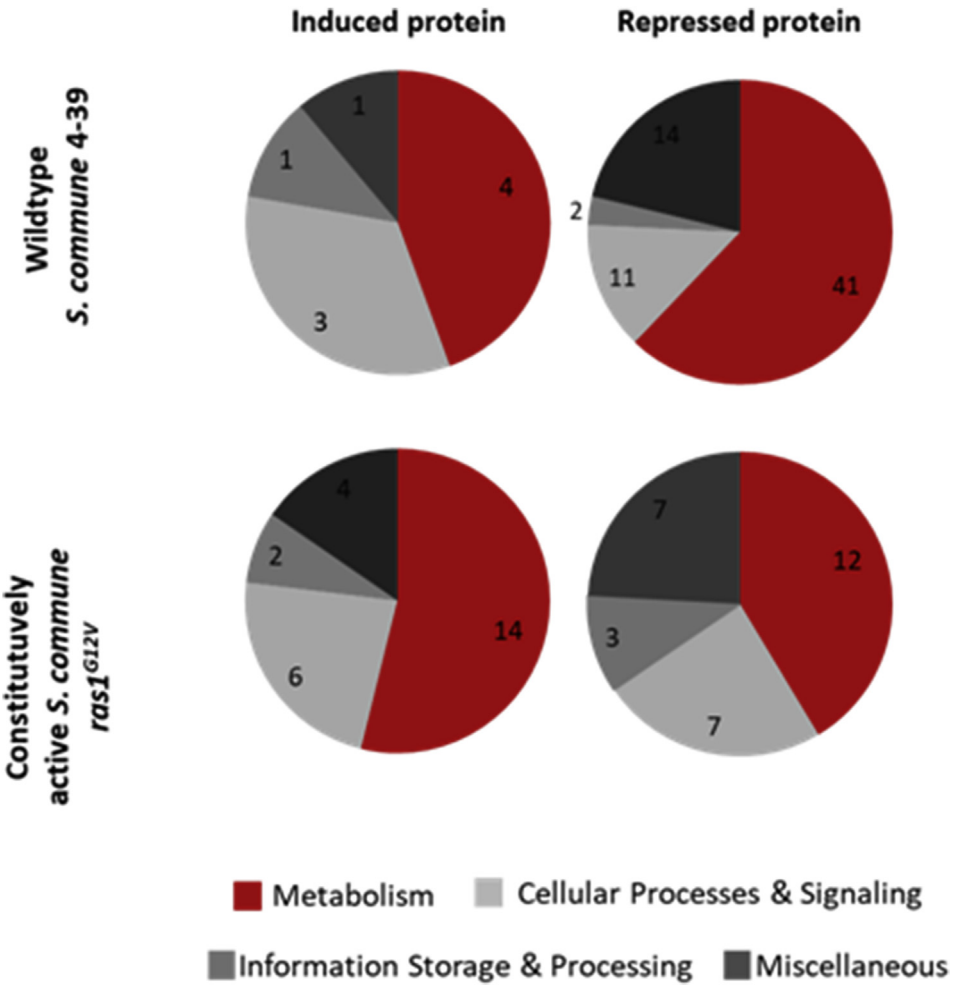

Fig. 5. KOG annotation for proteins regulated by lithium. *S. commune* 4–39 and *S. commune ras1*^{G12V} induced and repressed proteome changes are presented.

4. Discussion

Our study revealed an unprecedented crosstalk between Ras signaling and inositol phosphate signaling in the basidiomycete *S. commune*. Ras1 plays a versatile role in vegetative growth and sexual development of the fungus. We envisage that some of these functions are regulated through the transcriptional control exercised by Ras1 over *imp1*. Working with *S. commune,* we revealed a distinctive inhibitory effect of lithium on IMPase with dramatic and never before recorded alteration of inositol phosphates metabolism. It is important to note that IMPase of *S. commune* shares high similarity to other lithium-sensitive IMPases (suppl. Fig. S4), especially in the three common motifs that play critical roles in substrate binding, metal interaction, and nucleophilic activation interactions (York et al., 1995; Saxena et al., 2013).

The effect of lithium on fungal growth has been tested previously (Wildman, 1991; Dias Nunes et al., 2014). Growth rate inhibition of *S. commune* by lithium was highly associated with an alteration in hyphal morphology, consistent with the previously reported effects of lithium on white-rot basidiomycete fungi (Wildman, 1991; Dias Nunes et al., 2014). However, none of these studies linked the effects observed to IPs signaling. In the ascomycete yeasts *S. cerevisiae* and *S. pombe*, as well as in the basidiomycete yeast form of *C. neoformans*, the inhibition of IMPase by lithium induced an elevation of IP_1 levels, while there was no accumulation of IP_6 (Navarro-Avino et al., 2003). In *S. commune*, however, lithium modulated IPs metabolism in a different fashion. In *S. commune*, lithium decreased the level of IP_1 and significantly increased the levels of the highly phosphorylated inositol phosphates from IP_3 to IP_8.

Conversely, Ras1 activation in the *ras1*^{G12V} mutant dramatically repressed *imp1* expression, precluding lithium IMPase inhibition. Hampering *imp1* transcription or the pharmacological blockage of IMPase activity should in theory have similar biochemical consequences. However, only in wild-type cells lithium inhibition of IMPase led to a dramatic increase of higher phosphorylated IPs species. Histidine acid phosphatase (HAP), hydrolyzing IP_6 to lower phosphorylated inositol phosphates, is repressed upon lithium treatment in wildtype *S. commune*, allowing for the accumulation of IP_6 and inositol pyrophosphates. This phosphatase, however, is

specifically induced in the constitutively active *ras1*^{G12V} mutant. As a result, the dephosphorylation of highly phosphorylated species of IPs to inositol is enhanced, and the accumulation of higher phosphorylated inositol species was not observed.

The lithium depletion hypothesis (Berridge, 1989) proposes that the blockage of PLC generated IP_3 recycling to inositol has as consequence the depletion of cellular inositol pools. It also implicitly suggests that if IP_3 is not recycled, it could become substrate of kinases leading to the synthesis of higher phosphorylated IPs. Using *S. commune,* we were able to verify this expected effect of lithium on inositol metabolism, in contrast to other experimental models such *S. cerevisiae* where elevated IP_1 levels were the only observed response to lithium. Similar to the budding yeast, IP_1 was increased upon lithium action in mammalian neurons, both within the axons and the cell bodies (Andreassi et al., 2010). It is noteworthy to mention that the routine 24-h lithium treatment as usually evaluated in laboratory settings do not mimic the far longer (weeks) lithium therapeutic time-frame necessary to be beneficial to bipolar disorder patients. Therefore, although technically challenging, it will be important to evaluate, in future studies, the inositol phosphate profile of neurons treated with lithium for one or more weeks to verify, if the elevation of highly phosphorylated inositol species also occurs in mammalian neurons.

Proteome analysis showed a connection between IPs signaling, metabolic responses and cellular processes. The expression changes of kinases, fructose 1,6-bisphosphate aldolase, fructose-1,6-bisphosphatase, and actin illustrated the importance of IPs in this filamentous fungus that had not been seen previously. The changes in growth and hyphal morphology may be tracked back to actin expression changes upon lithium treatment, which effects mitosis, fruiting body development and meiosis in addition to the observed hyphal morphology changes (Jung et al., 2018). The ATPase repression in the wildtype under lithium treatment is in line with the previous studies showing that inositol depletion is responsible for vacuolar defect and the decrease of vacuolar ATPase (Deranieh et al., 2015).

S. commune with its unique physiology might provide new investigative opportunities to further elucidate the effect of lithium on IPs metabolism. The knockout of *imp1* could be useful to this end. However, *S. commune imp1* is expected to be essential (unpublished observation). Therefore, the study of transcriptional repression of *imp1* in the constitutively active *ras1*^{G12V} mutant and lithium enzymatic inhibition of IMPase provides the missing background. *S. commune* shares similar lithium regulatory mechanism with other organisms. However, its unique physiology might provide new analytical prospectives to clarify the effect of lithium and to pinpoint its mechanism of action in bipolar disorder.

5. Conclusions

Signaling pathways crosstalk are fundamental to fine tune physiological responses. Inositol phosphates constitute one of the most sophisticated signaling pathways, while small GTPase Ras regulated pathways are also very important to control cellular functions. Using *Schizophyllum commune,* we revealed a crosstalk between Ras1 and inositol phosphates. Ras1 mediated the repression of inositol monophosphatase (IMPase) transcription. A repression of the enzyme by lithium induced a considerable metabolic shift, leading to a massive increase in the level of higher phosphorylated inositol species. This metabolic change is implied by the lithium depletion hypothesis, but has remained unobserved so far. Proteome profiles were used to further link lithium action to changes in metabolism and cellular signaling. We provide new prospectives to elucidate the effect of lithium and to pinpoint its mechanism of action using a fungal model.

Declaration of interest

None.

Acknowledgments

This research was funded by International Leibniz Research School (ILRS) within the frame of GSC124 (JSMC), and by the CRC ChemBioSys funded through the Deutsche Forschungsgemeinschaft. We would like to thank Maria Pötsch for MALDI-TOF/TOF-analysis and Silke Steinbach for technical assistance. Inositol phosphate analyses were supported by support to the MRC/UCL Laboratory for Molecular Cell Biology University Unit (MC_UU_12018/4).

Appendix A. Supplementary data

Supplementary data to this article can be found online at https://doi.org/10.1016/j.jbior.2019.01.001.

References

Allison, J.H., Stewart, M.A., 1971. Reduced brain inositol in lithium-treated rats. Nat. New Biol. 233, 267–268.

Andreassi, C., Zimmermann, C., Mitter, R., Fusco, S., De Vita, S., Saiardi, A., Riccio, A., 2010. An NGF-responsive element targets myo-inositol monophosphatase-1 mRNA to sympathetic neuron axons. Nat. Neurosci. 13, 291–301.

Azevedo, C., Saiardi, A., 2006. Extraction and analysis of soluble inositol polyphosphates from yeast. Nat. Protoc. 1, 2416–2422.

Azevedo, C., Saiardi, A., 2017. Eukaryotic phosphate homeostasis: the inositol pyrophosphate perspective. Trends Biochem. Sci. 42, 219–231.

Banfic, H., Crljen, V., Lukinovic-Skudar, V., Dembitz, V., Lalic, H., Bedalov, A., Visnjic, D., 2016. Inositol pyrophosphates modulate cell cycle independently of alteration in telomere length. Adv. Biol. Regul. 60, 22–28.

Baykov, A.A., Evtushenko, O.A., Avaeva, S.M., 1988. A malachite green procedure for orthophosphate determination and its use in alkaline phosphatase-based enzyme

immunoassay. Anal. Biochem. 171, 266–270.
Berridge, M.J., 1989. The Albert Lasker medical awards. Inositol trisphosphate, calcium, lithium, and cell signaling. J. Am. Med. Assoc. 262, 1834–1841.
Berridge, M.J., Downes, C.P., Hanley, M.R., 1982. Lithium amplifies agonist-dependent phosphatidylinositol responses in brain and salivary glands. Biochem. J. 206, 587–595.
Bordier, C., 1981. Phase separation of integral membrane proteins in Triton X-114 solution. J. Biol. Chem. 256, 1604–1607.
Bradford, M.M., 1976. A rapid and sensitive method for the quantitation of microgram quantities of protein utilizing the principle of protein-dye binding. Anal. Biochem. 72, 248–254.
Brunsch, M., Schubert, D., Gube, M., Ring, C., Hanisch, L., Linde, J., Krause, K., Kothe, E., 2015. Dynein heavy chain, encoded by two genes in agaricomycetes, is required for nuclear migration in *Schizophyllum commune*. PLoS One 10, e0135616.
Cordeiro, C.D., Saiardi, A., Docampo, R., 2017. The inositol pyrophosphate synthesis pathway in *Trypanosoma brucei* is linked to polyphosphate synthesis in acidocalcisomes. Mol. Microbiol. 106, 319–333.
Crocco, P., Saiardi, A., Wilson, M.S., Maletta, R., Bruni, A.C., Passarino, G., Rose, G., 2016. Contribution of polymorphic variation of inositol hexakisphosphate kinase 3 (IP6K3) gene promoter to the susceptibility to late onset Alzheimer's disease. Biochim. Biophys. Acta 1862, 1766–1773.
Cryns, K., Shamir, A., van Acker, N., Levi, I., Daneels, G., Goris, I., Bouwknecht, J.A., Andries, L., Kass, S., Agam, G., Belmaker, H., Bersudsky, Y., Steckler, T., Moechars, D., 2008. IMPA1 is essential for embryonic development and lithium-like pilocarpine sensitivity. Neuropsychopharmacology 33, 674–684.
De Craene, J.O., Bertazzi, D.L., Bar, S., Friant, S., 2017. Phosphoinositides, major actors in membrane trafficking and lipid signaling pathways. Int. J. Mol. Sci. 18, 634.
Deranieh, R.M., Shi, Y., Tarsio, M., Chen, Y., McCaffery, J.M., Kane, P.M., Greenberg, M.L., 2015. Perturbation of the vacuolar ATPase: a novel consequence of inositol depletion. J. Biol. Chem. 290, 27460–27472.
Di Paolo, G., De Camilli, P., 2006. Phosphoinositides in cell regulation and membrane dynamics. Nature 443, 651–657.
Dias Nunes, M., Cardoso, L.W., Luz, J., Kasuya, M.C., 2014. Lithium chloride affects mycelial growth of white rot fungi: fungal screening for Li-enrichment. Afr. J. Microbiol. Res. 8, 2111–2123.
Erdmann, S., Freihorst, D., Raudaskoski, M., Schmidt-Heck, W., Jung, E.-M., Senftleben, D., Kothe, E., 2012. Transcriptome and functional analysis of mating in the basidiomycete *Schizophyllum commune*. Eukaryot. Cell 11, 571–589.
Gillaspy, G.E., 2011. The cellular language of myo-inositol signaling. New Phytol. 192, 823–839.
Gupta, S., Bhar, A., Chatterjee, M., Ghosh, A., Das, S., 2017. Transcriptomic dissection reveals wide spread differential expression in chickpea during early time points of *Fusarium oxysporum* f. sp. ciceri Race 1 attack. PLoS One 12, e0178164.
Hammond, G.R., Balla, T., 2015. Polyphosphoinositide binding domains: key to inositol lipid biology. Biochim. Biophys. Acta 1851, 746–758.
Hatch, A.J., Odom, A.R., York, J.D., 2017. Inositol phosphate multikinase dependent transcriptional control. Adv. Biol. Regul. 64, 9–19.
Irvine, R.F., Schell, M.J., 2001. Back in the water: the return of the inositol phosphates. Nat. Rev. Mol. Cell Biol. 2, 327–338.
Jung, E.-M., Kothe, E., Raudaskoski, M., 2018. The making of a mushroom: mitosis, nuclear migration and the actin network. Fungal Genet. Biol. 111, 85–91.
Kalujnaia, S., McVee, J., Kasciukovic, T., Stewart, A.J., Cramb, G., 2010. A role for inositol monophosphatase 1. IMPA1. in salinity adaptation in the euryhaline eel (*Anguilla anguilla*). Faseb. J. 24, 3981–3991.
Knabe, N., Jung, E.-M., Freihorst, D., Hennicke, F., Horton, J.S., Kothe, E., 2013. A central role for Ras1 in morphogenesis of the basidiomycete *Schizophyllum commune*. Eukaryot. Cell 12, 941–952.
Kothe, E., 1999. Mating types and pheromone recognition in the homobasidiomycete *Schizophyllum commune*. Fungal Genet. Biol. 27, 146–152.
Lev, S., Li, C., Desmarini, D., Saiardi, A., Fewings, N.L., Schibeci, S.D., Sharma, R., Sorrell, T.C., Djordjevic, J.T., 2015. Fungal inositol pyrophosphate IP_7 is crucial for metabolic adaptation to the host environment and pathogenicity. mBio 6, e00531-15.
Li, L., Wang, F., Yan, P., Jing, W., Zhang, C., Kudla, J., Zhang, W., 2017. A phosphoinositide-specific phospholipase C pathway elicits stress-induced Ca^{2+} signals and confers salt tolerance to rice. New Phytol. 214, 1172–1187.
Lonetti, A., Szijgyarto, Z., Bosch, D., Loss, O., Azevedo, C., Saiardi, A., 2011. Identification of an evolutionarily conserved family of inorganic polyphosphate endopolyphosphatases. J. Biol. Chem. 286, 31966–31974.
Mullaney, E.J., Ullah, A.H.J., 2005. Conservation of cysteine residues in fungal histidine acid phytases. Biochem. Biophys. Res. Commun. 328, 404–408.
Nanjareddy, K., Arthikala, M.K., Gomez, B.M., Blanco, L., Lara, M., 2017. Differentially expressed genes in mycorrhized and nodulated roots of common bean are associated with defense, cell wall architecture, N metabolism, and P metabolism. PLoS One 12, e0182328.
Navarro-Aviñó, J.P., Bellés, J.M., Serrano, R., 2003. Yeast inositol mono- and trisphosphate levels are modulated by inositol monophosphatase activity and nutrients. Biochem. Biophys. Res. Commun. 302, 41–45.
Nourbakhsh, A., Collakova, E., Gillaspy, G.E., 2015. Characterization of the inositol monophosphatase gene family in *Arabidopsis*. Front. Plant Sci. 5, 725.
Ohm, R.A., de Jong, J.F., Lugones, L.G., Aerts, A., Kothe, E., Stajich, J.E., de Vries, R.P., Record, E., Levasseur, A., Baker, S.E., Bartholomew, K.A., Coutinho, P.M., Erdmann, S., Fowler, T.J., Gathman, A.C., Lombard, V., Henrissat, B., Knabe, N., Kües, U., Lilly, W.W., Lindquist, E., Lucas, S., Magnuson, J.K., Piumi, F., Raudaskoski, M., Salamov, A., Schmutz, J., Schwarze, F.W.M.R., vanKuyk, P.A., Horton, J.S., Grigoriev, I.V., Wösten, H.A.B., 2010. The genome sequence of *Schizophyllum commune*. Nat. Biotechnol. 28, 957–965.
Palmer, G.E., Horton, J.S., 2006. Mushrooms by magic: making connections between signal transduction and fruiting body development in the basidiomycete fungus *Schizophyllum commune*. FEMS Microbiol. Lett. 262, 1–8.
Pan, L., Yang, Z., Wang, J., Wang, P., Ma, X., Zhou, M., Li, J., Gang, N., Feng, G., Zhao, J., Zhang, X., 2017. Comparative proteomic analyses reveal the proteome response to short-term drought in Italian ryegrass (*Lolium multiflorum*). PLoS One 12, e0184289.
Pfaffl, M.W., 2001. A new mathematical model for relative quantification in real-time RT-PCR. Nucleic Acids Res. 29 e45.
Raper, J.R., Miles, P.G., 1958. The genetics of *Schizophyllum commune*. Genetics 43, 530–546.
Saiardi, A., 2012. How inositol pyrophosphates control cellular phosphate homeostasis? Adv. Biol. Regul. 52, 351–359.
Saiardi, A., Mudge, A.W., 2018. Lithium and fluoxetine regulate the rate of phosphoinositide synthesis in neurons: a new view of their mechanisms of action in bipolar disorder. Transl. Psychiatry 8, 175.
Saiardi, A., Azevedo, C., Desfougères, Y., Portela-Torres, P., Wilson, M.S.C., 2018. Microbial inositol polyphosphate metabolic pathway as drug development target. Adv. Biol. Regul. 67, 74–83.
Saiardi, A., Sciambi, C., McCaffery, J.M., Wendland, B., Snyder, S.H., 2002. Inositol pyrophosphates regulate endocytic trafficking. Proc. Natl. Acad. Sci. U.S.A. 99, 14206–14211.
Saxena, S.C., Salvi, P., Kaur, H., Verma, P., Petla, B.P., Rao, V., Kamble, N., Majee, M., 2013. Differentially expressed myo-inositol monophosphatase gene (CaIMP) in chickpea (*Cicer arietinum* L) encodes a lithium-sensitive phosphatase enzyme with broad substrate specificity and improves seed germination and seedling growth under abiotic stresses. J. Exp. Bot. 64, 5623–5639.
Schubert, D., Raudaskoski, M., Knabe, N., Kothe, E., 2006. Ras GTPase-activating protein Gap1 of the homobasidiomycete *Schizophyllum commune* regulates hyphal growth orientation and sexual development. Eukaryot. Cell 5, 683–695.
Schwalb, M.N., Miles, P.G., 1967. Morphogenesis of *Schizophyllum commune*. II. Effect of microaerobic growth. Mycologia 59, 610–622.
Sherman, W.R., Leavitt, A.L., Honchar, M.P., Hallcher, L.M., Phillips, B.E., 1981. Evidence that lithium alters phosphoinositide metabolism: chronic administration elevates primarily D-myo-inositol-1-phosphate in cerebral cortex of the rat. J. Neurochem. 36, 1947–1951.
Shevchenko, A., Wilm, M., Vorm, O., Mann, M., 1996. Mass spectrometric sequencing of proteins silver-stained polyacrylamide gels. Anal. Chem. 68, 850–858.
Szijgyarto, Z., Garedew, A., Azevedo, C., Saiardi, A., 2011. Influence of inositol pyrophosphates on cellular energy dynamics. Science 334, 802–805.
Tsui, M.M., York, J.D., 2010. Roles of inositol phosphates and inositol pyrophosphates in development, cell signaling and nuclear processes. Adv. Enzym. Regul. 50, 324–337.
Wild, R., Gerasimaite, R., Jung, J.Y., Truffault, V., Pavlovic, I., Schmidt, A., Saiardi, A., Jessen, H.J., Poirier, Y., Hothorn, M., Mayer, A., 2016. Control of eukaryotic phosphate homeostasis by inositol polyphosphate sensor domains. Science 352, 986–990.
Wildman, H.G., 1991. Lithium chloride as a selective inhibitor of *Trichoderma* species on soil isolation plates. Mycol. Res. 95, 1364–1368.

Wilson, M.S., Livermore, T.M., Saiardi, A., 2013. Inositol pyrophosphates: between signalling and metabolism. Biochem. J. 452, 369–379.
Wyss, M., Brugger, R., Kronenberger, A., Remy, R., Fimbel, R., Oesterhelt, G., van Loon, A.P., 1999. Biochemical characterization of fungal phytases. myo-inositol hexakisphosphate phosphohydrolases.: catalytic properties. Appl. Environ. Microbiol. 65, 367–373.
Xie, N., Ruprich-Robert, G., Chapeland-Leclerc, F., Coppin, E., Lalucque, H., Brun, S., Debuchy, R., Silar, P., 2017. Inositol-phosphate signaling as mediator for growth and sexual reproduction in *Podospora anserina*. Dev. Biol. 429, 285–305.
York, J.D., Majerus, P.W., 1990. Isolation and heterologous expression of a cDNA encoding bovine inositol polyphosphate 1-phosphatase. Proc. Natl. Acad. Sci. U.S.A. 87, 9548–9552.
York, J.D., Ponder, J.W., Majerus, P.W., 1995. Definition of a metal-dependent/Li^+-inhibited phosphomonoesterase protein family based upon a conserved three-dimensional core structure. Proc. Natl. Acad. Sci. U.S.A. 92, 5149–5153.
Zhang, S.X., Duan, L.H., He, S.J., Zhuang, G.F., Yu, X., 2017. Phosphatidylinositol 3,4-bisphosphate regulates neurite initiation and dendrite morphogenesis via actin aggregation. Cell Res. 27, 253–273.